INFLUENCE OF ROTATIONAL OSCILLATION OF A CYLINDER IN THE INHERENT PARAMETERS OF THE FLOW

Silva, A. R., calicers@hotmail.com
Federal University of Uberlândia, School of Mechanical Engineering
2121, João Naves de Ávila Av, Santa Mônica District, zip code 38400-902, Uberlândia-MG, Brazil

Lima e Silva, A. L. F., alfsilva@unifei.edu.br
Federal University of Itajubá, School of Mechanical Engineering
1303 BPA Av., Pinheirinho District, zip code 37500-903, Itajubá-MG, Brazil.

Silveira-Neto A. aristeus@mecanica.ufu.br
Federal University of Uberlândia, School of Mechanical Engineering
2121, João Naves de Ávila Av, Santa Mônica District, zip code 38400-902, Uberlândia-MG, Brazil

Abstract. *In this paper the rotational oscillation of a cylinder is numerically studied. The two-dimensional Navier-Stokes equations for incompressible fluids with the Smagorinsky sub-scale model are solved for a cartesian non-uniform grid. The Immersed Boundary Method with Virtual Physical Model are used for modelling the presence of the circular cylinder. The simulations were carried out for a Reynolds number equal to 1000 for different amplitudes of oscillation and different forcing frequencies. In order to better understand the flow dynamics due to the rotational oscillation movement of the cylinder, the aerodynamic coefficients, the Strouhal number and the length of the recirculation are presented.*

Keywords*: rotational-oscillation, cylinder, amplitude, forcing frequency.*

1. INTRODUCTION

The flow around a circular cylinder has been a topic of interest for many years mainly due to the importance of an engineering problem of vortex induced vibration of bluff bodies in a stream. Vortex streets are formed in the wake of a bluff body over a wide range of Reynolds number. The formation of the vortices in the flow past a stationary circular cylinder has been well documented, both numerically and experimentally (e.g., Lima e Silva, 2002; Silva, 2004; Lai and Peskin, 2000; Ryan et al. 2004; Su et al. 2006). A number of researchers has studied the effects of rotating cylinder on the wake structure (e.g., Silva et al. 2004a, Silva et al., 2004b, Carvalho, 2003, Kang et al., 1999). Flows over a bundle of cylinders disposed in "*V*", at different angles were also studied by Silva et al. (2003) for low Reynolds number.

The effective control of drag exerted by the fluid on the cylinder has been a challenge that has received particular attention. The drag force on the cylinder may be reduced by an active control in the rotational oscillation of the cylinder. The literature covers the effect of cross-flow oscillations and in-line oscillations, but studies on rotational oscillations are very few. According to Fujisawa et al. (1998), the effects of rotational oscillations on the cylinder wake were first studied by Okajima et al. (1975).

The purpose of the present paper is to study the influence of rotational oscillation on the flow around a circular cylinder in a uniform flow.

2. MATHEMATICAL METHODOLOGY AND NUMERICAL METHOD

All the simulations were carried out using the Immersed Boundary Method (Peskin, 1977) with the Virtual Physical Model (Lima e Silva, 2002).

The Navier-Stokes equations and continuity can be written as follow:

$$\frac{\partial u_i}{\partial t} + \frac{\partial \left(u_i u_j \right)}{\partial x_j} = -\frac{1}{\rho}\frac{\partial p}{\partial x_j} + \frac{\partial}{\partial x_j}\left[\nu_{ef} \left(\frac{\partial u_i}{\partial x_j} + \frac{\partial u_j}{\partial x_i} \right) \right] + f_i \tag{1}$$

$$\frac{\partial u_i}{\partial x_i} = 0 \tag{2}$$

where ρ e ν_{ef} are the specific mass and effective viscosity, respectively, u_i, represents the components of the velocity, p is the pressure and f_i the components of eulerian force vector. The force term is calculated by the distribution of the components of lagrangian vector as follow:

$$\vec{f}\left(\vec{x}\right) = \sum_k D_{ij}\left(\vec{x} - \vec{x}_k\right)\vec{F}\left(\vec{x}_k\right)\Delta S^2\left(\vec{x}_k\right) \tag{3}$$

where $\vec{x}$ and $\vec{x}_k$ are the position vectors of the eulerian and lagrangian points, respectively, ΔS is the distance between two lagrangian points, $\vec{F}\left(\vec{x}_k\right)$ is the interfacial lagrangian force and D_{ij} is the interpolation/distribution function, proposed by Juric (1996).

The turbulence model used in the present work is based in the filter process, named by box filter described in Silveira-Neto et al. (2002) and Silveira-Neto (2003). The turbulent viscosity (Smagorinsky, 1963) is given as a function of the strain rate and scale length as:

$$\nu_t = \left(C_S \ell\right)^2 \sqrt{2\overline{S_{ij}}\,\overline{S_{ij}}} \tag{4}$$

$$\overline{S_{ij}} = \frac{1}{2}\left(\frac{\partial \overline{u_i}}{\partial x_j} + \frac{\partial \overline{u_j}}{\partial x_i}\right) \tag{5}$$

where $\ell = \sqrt{\Delta x \Delta y}$ is the characteristic sub-grid length, $\overline{S_{ij}}$ is the strain rate and C_S is the Smagorinsky constant. The analytical value $C_S = 0.18$, which was determined by Lilly (1967), was used.

In all of the simulations a damping function was used in the outlet of the domain. Details of this procedure can be found in Silva (2004), Silva et al. 2004c and Souza et al. (2002).

The Fractional Step Method (Chorin, 1968) based on the pressure correction was also used. The spatial discretization of the Navier-Stokes equations was done by the Finite Difference Method and the time discretization by the second order Runge-Kutta method. The effective viscosity and velocities were interpolated as suggested by Patankar (1980).

3. RESULTS AND DISCUSSION

The influence of the forced frequency and the oscillation amplitude in the structure wake, in the behavior of the aerodynamic coefficients as drag and lift, in the length of recirculation bubble and in the Strouhal number were analyzed. The results are presented for different frequencies, $0.2 \le f_c / f_o \le 6.0$ (f_c is the forced frequency and f_o is the natural frequency of vortex shedding for stationary cylinder) and amplitudes $1.0 \le A \le 3.0$ (A is the oscillation amplitude). The Reynolds number based on the diameter of the cylinder and on the free stream velocity is *1000* and the dimension of the domain is 40 x 15m. All the simulations were done with a non-uniform grid of *400 x 125* points, where the small space grid in the normal and transversal directions of the flow is given by $2R/nmc$ (nmc is the grid number inside the cylinder). The cylinder was located at *16.5d* in *x* direction and *7.5d* in *y* direction, where *d* is the diameter of the cylinder.

The behavior of structure wake is different when the cylinder oscillates around its own axis. According to Ponta and Aref (2006), the usual vortices wake would be designed as '2S' mode in the classification of WR (Williamson-Roshko). This mode indicates the vortex shedding of two single vortices per cycle of each side of the cylinder. There are five different flow regimes according to Lee and Lee (2006), for a amplitude equal 30°. Many other authors consider only two different regimes to classify the flow, named non lock-on and lock-on regimes (Cheng et al., 2001; Cheng et al., 2001a).

3.1. Description of the flow

The oscillation amplitude and frequency were used as control parameters. The tangential velocity over the cylinder is given as:

$$V_t\left(t\right) = AR\sin\left(2\pi f_c t\right) \tag{6}$$

where $A = \dfrac{R\omega_{máx}}{U_\infty}$ is the oscillation amplitude, R is the radius of cylinder and t is the physical time of the simulation. According to He et al. (2000) this procedure is constituted by two degrees of freedom.

3.2. Vorticity Fields

Figure 1 shows the vorticity fields for an admensional time of 200, $0.2 \le f_c / f_o \le 6.0$ and $1.0 \le A \le 3.0$. The positive vorticity is represented by the red color and the negative vorticity by the blue color. The three columns represent the simulations with $A = 1$, $A = 2$ and $A = 3$, respectively. As can be observed there are different modes of vortex shedding for a given column and for the same frequencies considering different amplitudes.

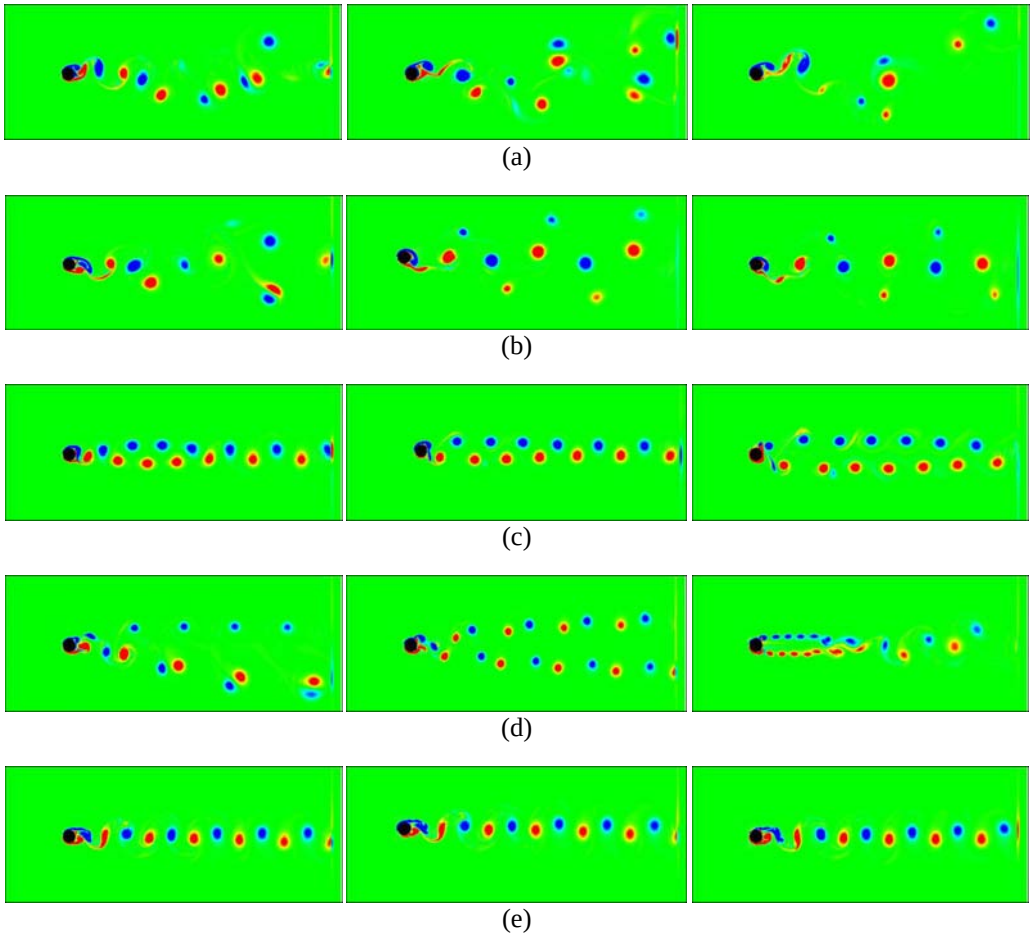

Figure 1. Vorticity field: a) $f_c = 0.2 f_o$; b) $f_c = 0.5 f_o$; c) $f_c = 0.9 f_o$; d) $f_c = 2.5 f_o$; e) $f_c = 6.0 f_o$. From left to right $A = 1$, $A = 2$ and $A = 3$

For $f_c = 0.2 f_o$ and $A = 1$, vortices are generated from both sides of the cylinder and the wake oscillates with time. There are pairs of vortices with opposed signs in the wake. This behavior was also observed in the other amplitudes, however the longitudinal and transversal displacement between the pairs of vortices is larger. For the frequency $f_c = 0.5 f_o$, the behavior is similar to the previous one, however for $A = 3$, the pairs of vortices have the same signal. For $f_c = 0.9 f_o$, the vortices are synchronized with the oscillation of the cylinder. In other words, the cylinder and vortex shedding have the same characteristic frequency ($f_v = f_c$). This is the lock-on phenomenon or resonance. In this regime, the formation of an elliptic wake close to the cylinder with vortices of the same signal in the same row was observed. These vortices form a single wake far from the cylinder. The range of the lock-on regime obtained in this work for $A = 1$ was $0.6 \le f_c / f_o \le 1.05$, while for $A = 2$ was $0.5 \le f_c / f_o \le 1.1$ and for $A = 3$ was $0.2 \le f_c / f_o \le 1.8$.

For $f_c \le 2.8 f_o$ and $A = 1$, a transition from the vortex shedding mode to the 'P+S' mode was found, which is clear at $f_c = 2.5 f_o$ and $f_c = 2.8 f_o$ (not shown here). This mode corresponds to one pair of vortices of one side and a single vortex of the other side. It was also observed that the wake has the form of a cone. This structure wake is also observed for $A = 2$ for the same frequency. However in this case, the vortex shedding mode is named '2P', that is, two pairs of vortices in each cycle. Increasing the amplitude, $A = 3$, a double wake close to the cylinder and a single wake far away were noted. For all amplitudes analyzed and for the larger frequencies it were observed that the wake vortices come back to the regular configuration of the Kármán street and the standard of vortices do not change anymore. The non synchronized flow is similar to the flow for the stationary cylinder with some disturbance due to the movement

(Tuszynski and Löhner, 1998). In other words, the disturbance caused by the oscillation is limited near the cylinder, instead of downstream, the vortices reorganize to form the Von-Kármán street. This behavior is better visualized in the next item by the power spectra.

3.3. Drag coefficient

The control of the instabilities that lead to the vortex shedding is possible when the cylinder is forced to oscillate in the sinusoidal mode as Eq. 6. Figure 2 shows the behavior of the mean drag coefficient C_d versus the oscillation frequencies. The results were compared with the numerical results of Cheng et al. (2001a), Chou (1997) and Lu and Sato (1996).

The results of the present work are in good agreement with those of other authors in the resonance range. For high f_c / f_o, the results also tended to approximate to those of Cheng et al. (2001) for amplitudes 2 and 3. High C_d values in the lock-on regime and small values for high forced frequency, out of the lock-on regime were found. The mechanism of drag reduction is caused by the combined effect of forced frequency and oscillation amplitude due to the modification of wake at high frequency and of the delay in the separation of the flow. It is worth to note that the quantitative difference would be a consequence of the influence of the flow parameters, of the different numerical methods and of the assumptions adopted in the simulations. However, considering that at a given frequency, the vortices wake acquire the configuration and frequency of the classic Von Kármán street, it is expected that the value of drag would be close to the correspondent value of a stationary cylinder. This coherence can be observed in the results of the present work.

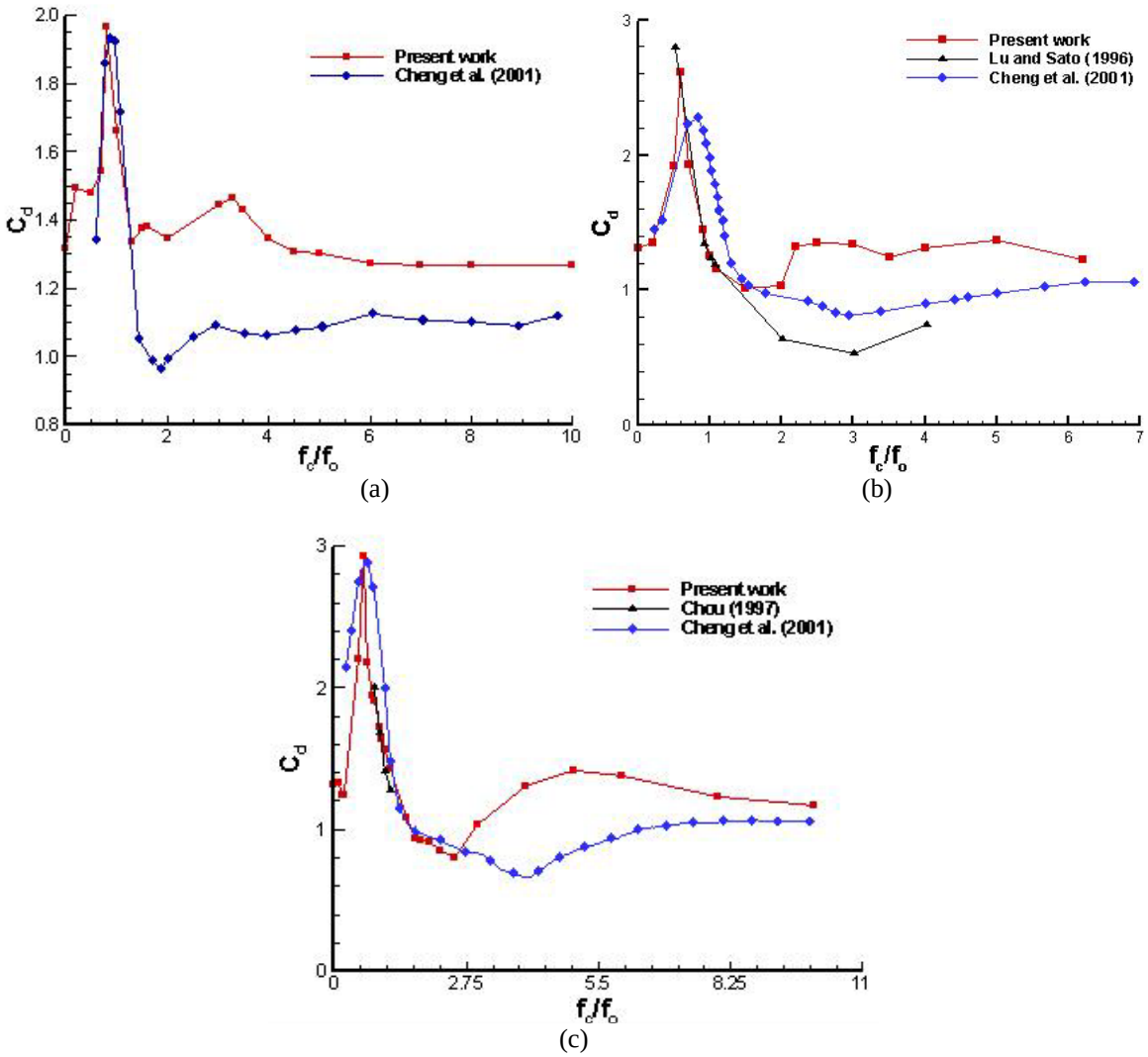

Figure 2. Mean drag coefficient: a) $A = 1$, b) $A = 2$ and c) $A = 3$

Figure 3 shows the behavior of the mean drag coefficient with the oscillation amplitude for the two frequencies. It is observed for $A = 1$ that the mean drag presented approximately the same value for both frequencies. Increasing the

oscillation amplitude an increase of the mean drag for low frequency and reduction for high frequency is observed. This behavior was already mentioned previously. Depending on the amplitude, the minimum drag can be around half or even a third of the stationary case value (Srinivas and Fujisawa, 2003). For Ray and Christofides (2005), when the cylinder oscillates at five times the natural frequency, it exhibits a drag reduction compared with the stationary case, to a range Reynolds number of 100 – 500.

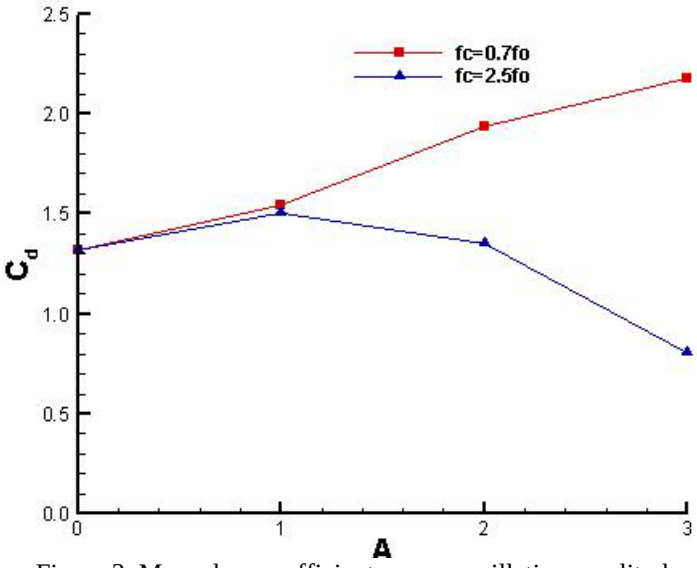

Figure 3. Mean drag coefficient versus oscillation amplitude

3.4. Power Spectra

The power spectra obtained by Fast Fourier Transform *(FFT)* of the lift coefficient signal is presented in Fig. 4 for the same ratios of frequency and amplitude of the previous item. The columns refer to the amplitudes $A=1$, $A=2$ and $A=3$, respectively.

For $A=1$ and $f_c \le 0.5 f_o$ there are two peaks of frequencies in the power spectra. One of them corresponds to the smallest frequency, that is, the forced frequency f_c and the other is the natural frequency of vortex shedding f_v which is near f_o (frequency of the stationary cylinder). In this range it can be noted that the smallest frequency has nearly the same magnitude for both ratio of frequency. In the lock-on regime only one peak is observed and the vortex shedding frequency f_v is synchronized with the forced frequency of cylinder f_c $(f_v \approx f_c)$. According to Lee and Lee (2006), as the oscillation amplitude decreases, the range of lock-on also decreases until reaching a given limit amplitude, which above this, the lock-on phenomenon only occur at $f_c = 1.0 f_o$. Increasing the frequency, the two peak reappear indicating that the lock-on no longer exists. For $f_c = 6.0 f_o$, the magnitude of the small scale frequency f_r increase and approaches of the value of the natural vortex shedding frequency.

For $A=2$, the range of lock-on regime is $0.5 \le f_c / f_o \le 1.1$. The magnitude of the peaks are greater than those of $A=1$. It was also observed a decrease in the magnitude of the frequency peak along the lock-on regime. For $f_c \le 2.5 f_o$ the value of the large scale vortex shedding frequency f_r is smaller than the value for the stationary cylinder. For $f_c \ge 3.0 f_o$, due to interaction between the vortices the final configuration has type and frequency f_r similar to the Von-Kármán of the stationary cylinder f_o.

The lock-on range, for $A=3$, occurs for $0.2 \le f_c / f_o \le 2.5$. For the same Reynolds number and amplitude, the range of lock-on regime found by Cheng et al (2001a) was $0.5 \le f_c / f_o \le 3.0$. It can be observed that the range of lock-on regime increase with the oscillation amplitude. For $f_c > 3.0 f_o$ the magnitude of lift fluctuating at the scale vortex shedding frequency tends to be constant, implicating in their stability. It was also noted that this frequency remains approximately at f_o for flow past a stationary cylinder. At high frequencies all the amplitudes presented the same behavior.

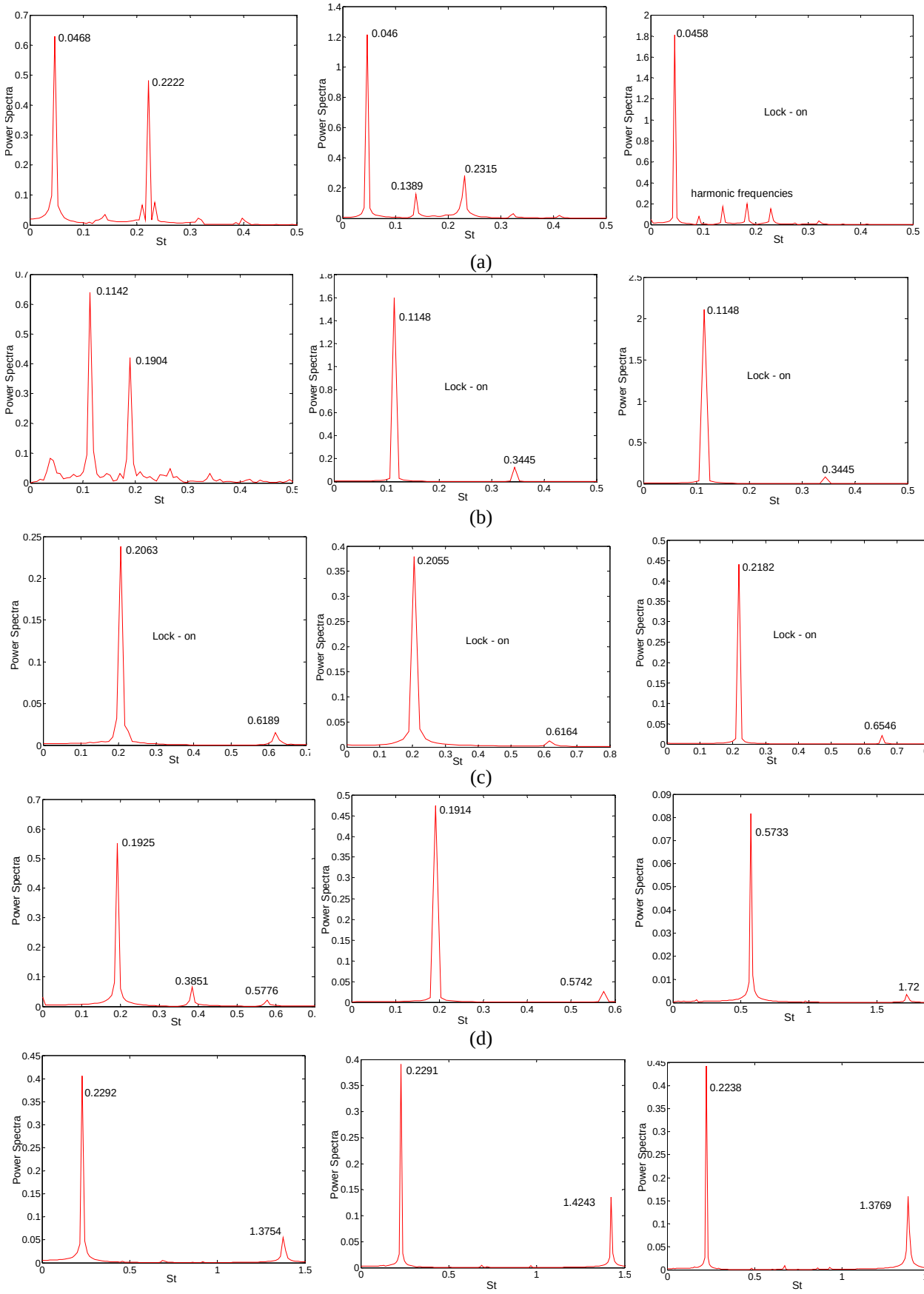

Figure 4. Power spectra: a) $f_c = 0.2\, f_o$; b) $f_c = 0.5\, f_o$; c) $f_c = 0.9\, f_o$; d) $f_c = 2.5\, f_o$; e) $f_c = 6.0\, f_o$ From left to right $A = 1$, $A = 2$ and $A = 3$.

3.5. Length of recirculation bubble.

The length of recirculation bubble L_w is defined as the distance between two stagnation points downstream of the cylinder. The first point is located at the surface of the cylinder and the second at the end of the bubble. For this reason many numerical probes were created downstream of cylinder, as presented in Fig. 5. The time average of the *y* component of the velocity was obtained at each probe. The distance between two points where the velocity is zero gives the value of L_w.

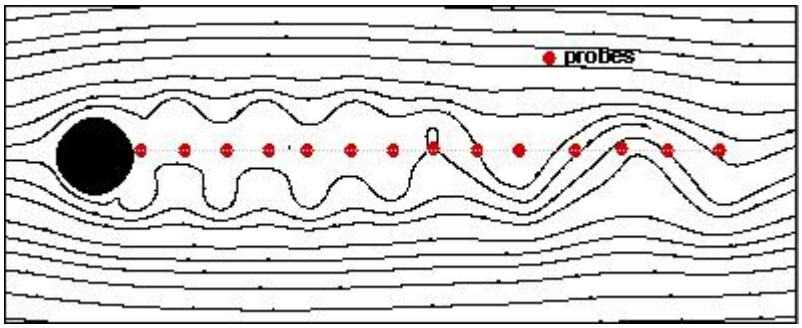

Figure 5. Illustrative scheme of the positions of the numerical probes.

Figure 6 shows the mean length of recirculation, formed downstream of the cylinder versus ratios of frequency for all analyzed amplitudes.

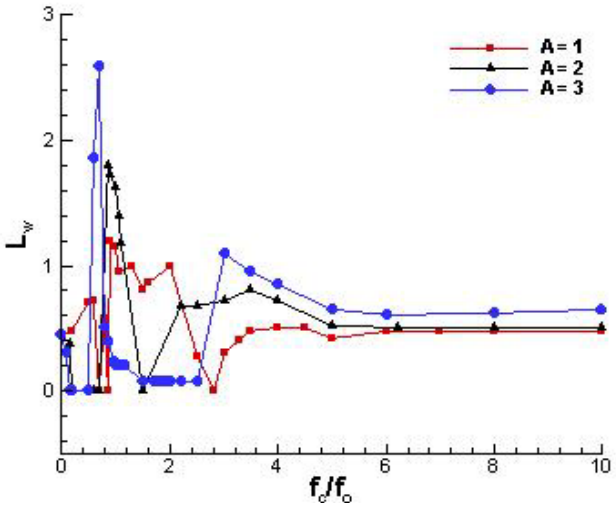

Figure 6. Mean length of recirculation bubble.

As can be noted by the presented results, the control parameters not only change the standard configuration of wake as they also alter the forces acting on the cylinder. It was also observed alterations in the length of recirculation bubble. For small frequencies where the flow is more accelerated it is noted a reduction on the length compared to the stationary case, $L_w = 0.45$. In the lock-in regime, it is observed an increase in drag due to the accelerated flow and it is also observed an increase in the length of recirculation. It is worth to emphasize that out of lock-on regime, where the forced frequency is greater than the natural frequency, the length of recirculation bubble is almost the same as the length of the stationary cylinder. This behavior is comparable with the observations found for vorticity field and drag coefficients.

4. CONCLUSIONS

In this work, the two-dimensional, incompressible viscous flow over a circular cylinder was examined with the effect of controlled rotational oscillation cylinder in reducing the drag and the influence in the Strouhal number and in the length of recirculation bubble. It was observed that the drag reduction is strengthened with an increase in oscillation amplitude, but it is saturated at higher oscillation amplitude. Thus, the mechanism of drag reduction is considered to be due to the combined effect of optimal pairs $\{A, f_c\}$, which is caused by the modification of the flow structure by generating small-scale vortices along the shear layers and the delay in mean separation points along the cylinder surface. The maximum drag reduction compared at the value of stationary cylinder was 38.8% at $A = 3$ and

$f_c = 1.65 f_o$, while at $A = 2$, $f_c = 2.5 f_o$ and $A = 1$, $f_c = 7 f_o$ the reduction were 24.13% and 3.76% respectively. With appropriate choice of the control parameters, the rotational oscillation of a cylinder can be a promising method for controlling the drag acting on the cylinder. Importantly for practical applications, this approach is effective even at large Reynolds numbers.

5. ACKNOWLEDGEMENTS

The authors gratefully acknowledge the support of CNPq, the Federal University of Uberlândia – UFU and FAPEMIG.

6. REFERENCES

Cheng, M., Liu, G.R. and Lam, K.Y.,2001, "Numerical simulation of flow past a rotationally oscillating cylinder". Computers & Fluids**.** 30, pp. 365-392.

Cheng, M., Chew, Y.T. and Luo, S. C.,2001a, "Numerical investigation of a rotationally oscillating cylinder in mean flow", Journal of Fluids and Structures**,** 15, pp. 981-1007.

Chorin, A., 1968, "Numerical solution of the Navier-Stokes equations", Math. Comp. 22, 745–762.

Chou, M.H, 1997, "Sinchronization of vortex shedding from a cylinder under rotary oscillation", Computers & Fluids**,** v. 36, n. 8, pp 755-774.

Fujisawa, N., Ikemoto, K. and Nagaya, K., 1998, "Vortex Shedding Resonance from a Rotationally Oscillating Cylinder", Journal of Fluids and Structures**,** 12, pp 1041-1053.

He, J.W., Glowinski, R., Metcalfe, R., Nordlander, A. and Periaux, J., 2000, "Active Control and Drag Optimization for Flow Past a Circular Cylinder I. Oscillatory cylinder Rotation", Journal of Computational Physics**.** 163, pp 83-117.

Juric, D., 1996, "Computation of phase change", Ph. D. Thesis - Mech. Eng. Univ. of Michigan, USA.

Kang, S., Choi, H. and Lee, S. C.,1999, "Laminar Flow past a Rotating Circular Cylinder", Physics of Fluid, 11, pp 3312-3320.

Lai, M-C. and Peskin, C.S., 2000, "An Immersed Boundary Method with Formal Second-Order Accuracy and Reduced Numerical Viscosity", Journal of Computational Physics**.** 160, pp 705-719.

Lee, S-J. and Lee, J-Y., 2006, Flow structure of wake behind a rotationally oscillating circular cylinder", Journal of Fluids and Structures, 22, pp. 1097-1112.

Lilly, D.K., 1967, "The representation of small-scale Turbulence in Numerical Experiments", *Proc. IBM Sci, Comp. Symp. Environ. Sci, IBM Data Process. Did., White Plains. NY*, pp 195-210.

Lima e Silva, A.L.F, 2002, "Desenvolvimento e Implementação de uma nova Metodologia para Modelagem de Escoamentos sobre Geometrias Complexas: Método da Fronteira Imersa com Modelo Físico Virtual", Tese de Doutorado – Universidade Federal de Uberlândia, Uberlândia.

Okajima, A., Takata, H. and Asanuma, T., 1975, "Viscous flow around a rotationally oscillating circular cylinder", Reports of Institute of Space and Aeronautical Science**.** University of Tokyo, n. 532, pp 311-338.

Patankar, S.V., 1980, "Numerical Heat Transfer and Fluid Flow", Taylor & Francis, 197p.

Peskin, C.S., 1977, "Numerical Analysis of Blood Flow in the Heart", Journal of Computational Physics**.** 25, pp 220-252.

Ponta, F.L. and Aref, H., 2006, "Numerical experiments on vortex shedding from an oscillating cylinder", Journal of Fluids and Structures, 22, pp. 327-344.

Ray, K., Prasenjit, and Christofides, D.P., 2005, "Control of flow over a cylinder using rotational oscillations". Computers and Chemical Engineering, 29, pp 877-885.

Ryan, K., Pregnalato, C.J., Thompson, M.C. and Hourigan, K., 2004, "Flow-induced vibrations of a tethered circular cylinder", Journal of Fluids and Structures. 19, pp 1085-1102.

Silva, A.R., 2004, "Simulação Numérica de Escoamentos em Transição sobre Cilindros Imersos**",** Dissertação de Mestrado. – Universidade Federal de Uberlândia, Uberlândia.

Silva, A.R., Lima e Silva, A.L.F. and Silveira-Neto, A.,2003, "Modelagem Matemática e simulação Numérica de escoamentos sobre bancos de cilindros imersos dispostos em diferentes ângulos", VI Congresso Íbero-Americano de Engenharia Mecânica, Coimbra-Portugal.

Silva, A.R., Carvalho, G.B., Lima e Silva, A.L.F., Mansur, S.S. and Silveira-Neto, A.,2004a, "Simulação Numérica de escoamentos sobre cilindros imersos com e sem rotação, utilizando-se o Método da Fronteira Imersa, VI Simpósio Mineiro de Mecânica Computacional, Itajubá – São Paulo.

Silva, A.R., Carvalho, G.B., Lima e Silva, A.L.F., Mansur, S.S. and Silveira-Neto, A.,2004b, "Modelagem Matemática e simulação Numérica de escoamentos sobre corpos móveis utilizando-se o Método da Fronteira Imersa", Proceedings of the 10º Brazilian Congress of Thermal Sciences and Engineering – ENCIT, Rio de Janeiro, Brazil.

Silva, A.R., Lima e Silva, A.L.F., Mansur, S.S. and Silveira-Neto, A.,2004c, "Experimentos numéricos utilizando diferentes esquemas de discretização temporal em modelagem da turbulência", Proceedings of the 10º Brazilian Congress of Thermal Sciences and Engineering – ENCIT, Rio de Janeiro, Brazil.

Silveira-Neto, A., Mansur, S.S., and Silvestrini, J.H., 2002, "Equações da Turbulência: Média versus filtragem", III Escola da Turbulência.

Silveira-Neto, A., 2003, "Apostila do curso de Turbulência".

Smagorinsky, J., 1963, "General Circulation Experiments with Primitive Equations", Mon. Weather Rev, v. 91, pp 99-164.

Souza, L.F., Mendonça, M.T., Medeiros, M.A. and Kloker, M., 2002, "Three Dimensional Code Validation for Transition Phenomena", III Escola de Turbulência.

Srinivas, K. and Fujisawa, N., 2003, "Effect of rotational oscillation upon fluid forces about a circular cylinder", Journal of Wind Engineering and Industrial Aerodynamics**,** 91, pp 637-652.

Su, S-W., Lai, M-C. and Lin, C-A., 2006, "An immersed boundary technique for simulating complex flows with rigid boundary", Computers & Fluids**.** Article in Press.

Tusynski, J. and Löhner, R., 1998, "Control of a Kármán Vortex Flow by Rotational Oscillations of a Cylinder", George Mason University**,** USA**.** 15, pp 1-12.